Wigner crystal versus Friedel oscillations in the one-dimensional Hubbard model

Stefan A. Söffing, Michael Bortz, Imke Schneider, Alexander Struck, Michael Fleischhauer, and Sebastian Eggert
Department of Physics and Research Center OPTIMAS, University of Kaiserslautern, D-67663 Kaiserslautern, Germany
(Received 2 April 2009; published 18 May 2009)

We analyze the fermion density of the one-dimensional Hubbard model using bosonization and numerical density matrix renormalization group calculations. For finite systems we find a relatively sharp crossover even for moderate short-range interactions into a region with $4k_F$ density waves as a function of density. The results show that the unstable fixed point of a spin-incoherent state can dominate the physical behavior in a large region of parameter space in finite systems. The crossover may be observable in ultracold fermionic gases in optical lattices and in finite quantum wires.

DOI: 10.1103/PhysRevB.79.195114 PACS number(s): 71.10.Pm, 37.10.Jk, 73.21.Hb

I. INTRODUCTION

Having been predicted in the early days of quantum mechanics, the Wigner crystal[1] is one of the simplest but most dramatic many-body effects: due to the long-range repulsive forces, electrons spontaneously form a self-organized lattice at low enough densities and temperatures much different from a free electron gas. Experimental verification has been difficult but very recently signatures of a Wigner crystal were reported in carbon nanotubes.[2] Using ultracold gases in optical lattices, it is now also possible to produce well-controlled correlated fermion systems in restricted dimensions, albeit with *short-range* interactions.[3,4]

The Wigner crystal in one dimension (1D) has been discussed so far mostly in the context of long-range interactions. In that case, it has been predicted by Schulz[5] that the density-density correlations corresponding to an equally spaced interparticle distance become dominant. A crossover to Wigner density waves has been observed numerically at strong long-range interactions with very few particles.[6] However, for short-range interacting fermion systems in 1D possible Wigner crystal signatures have not been addressed theoretically so far.

The prototypical model for short-range interacting fermions is the repulsive $(U>0)$ 1D Hubbard model

$$H = -t\sum_{x=1}^{L-1}(\psi_{\sigma,x}^{\dagger}\psi_{\sigma,x+1} + \text{H.c.}) + U\sum_{x=1}^{L} n_{\uparrow,x}n_{\downarrow,x}. \tag{1}$$

Even though many exact results have been derived for this model using the Bethe ansatz,[7] the local densities in finite chains with open boundaries cannot yet be calculated by exact methods.

It is known that at low energies the short-range interacting system in Eq. (1) becomes effectively scale invariant up to well-understood logarithmic corrections in the spin channel. Therefore, any crossover toward a different physical region would be unexpected. Moreover, a Wigner crystal region should be unstable since the $2k_F$-density Friedel oscillations[8] are always the slowest decaying correlations due to a bounded Luttinger parameter[5] $0.5 \le K_c \le 1$. Nonetheless, subdominant oscillations at other wave numbers also exist as has been explicitly shown, e.g., for the Hubbard model in a finite magnetic field.[9,10]

We now study the density distribution in finite Hubbard chains with hard-wall boundaries by a combination of bosonization and numerical density matrix renormalization group (DMRG) calculations. In Sec. II we describe how $2k_F$- and $4k_F$-density oscillations typically arise in 1D systems. The corresponding analytical expressions for the model (1) are derived using bosonization in Sec. III. Using the bosonization results, it is then possible to accurately analyze the numerical results in Sec. IV. The physical interpretations and conclusions are presented in Sec. V. Despite the fact that the interactions are short ranged and of moderate strength, we find that a region with dominant $4k_F$ oscillations is always stable at low filling. The results show that the scale invariance is explicitly broken. The observed Wigner crystal region illustrates that in 1D even short-range interactions have an increasing effect with *growing* interparticle spacing. The observed crossover is related to the so-called spin-incoherent Luttinger liquid.[11]

II. DENSITY OSCILLATIONS

The density profile in a system of interacting particles can be taken as a good indication of the nature of the ground state. For example, let us consider a true Wigner crystal in 1D with broken translational symmetry, where the particles are localized at regular distances. If the average filling is given by n_0, the corresponding density $n(x)$ would then be well described by a sum of Gaussian wave functions localized at positions $x=j/n_0$ with some localization length ξ

$$n(x) = \sum_{j=-\infty}^{\infty} \frac{1}{\sqrt{2\pi}\xi}\exp\left(-\frac{(x-j/n_0)^2}{2\xi^2}\right) = n_0\theta_3(\pi n_0 x, e^{-2\pi^2\xi^2 n_0^2}), \tag{2}$$

where we have used an exact identity for the elliptic Jacobi theta function $\theta_3(x,q) \equiv \Sigma_j q^{j^2} e^{2jix}$.

Interestingly, for a moderate particle distance in relation to the localization length $1/n_0 \lesssim 3\xi$, we have $e^{-2\pi^2\xi^2 n_0^2} \ll 1$ and the expression (2) is well approximated by a simple oscillation of the form

$$n(x) \approx n_0(1 + 2e^{-2\pi^2\xi^2 n_0^2}\cos(2\pi n_0 x)). \tag{3}$$

Since the Fermi point of a filled Fermi sea with density n_0 is given by $k_F = n_0\frac{\pi}{2}$ in the thermodynamic limit, it is clear that

 ©2009 The American Physical Society

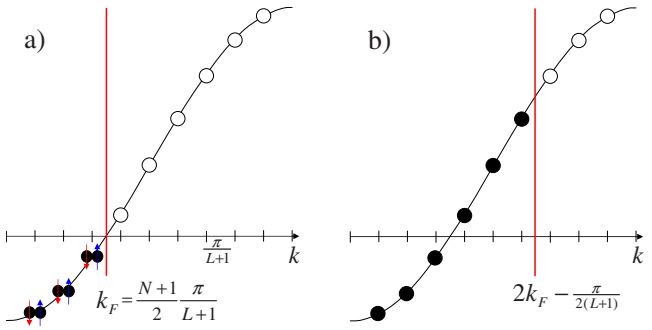

FIG. 1. (Color online) Schematic occupied states for (a) the nearly free case and (b) for strong interactions ("large Fermi sea").

the oscillations in Eq. (3) correspond to a $4k_F$ density wave. In this sense, $4k_F$ density oscillations and the Wigner crystal state can be taken to be equivalent phenomena. The amplitude of the oscillations in Eq. (3) can even be used to extract the effective localization length ξ.

There is, however, another possible reason for $4k_F$ oscillations in a finite system, which is linked to open boundary conditions and the arrangement of standing waves in momentum space. Due to interactions, fermions of opposite spin may no longer be allowed to occupy the same single-particle states and the Fermi sea is filled to effectively twice the original Fermi point relative to the noninteracting case as shown in Fig. 1. The summation over standing waves $\sin(n\frac{\pi}{L+1}x)$ results in a density of the form

$$n(x) = \frac{2}{L+1}\sum_{n=1}^{N}\sin^2\left(n\frac{\pi}{L+1}x\right) = n_0 - \frac{\sin\left(4k_F - \frac{\pi}{L+1}\right)x}{2(L+1)\sin\left(\frac{\pi}{L+1}x\right)}, \tag{4}$$

where we have used "open" boundary conditions $\psi_{\sigma,0} = \psi_{\sigma,L+1} = 0$ on a finite lattice with a lattice constant of unit length. The Fermi point $k_F = \frac{N+1}{2}\frac{\pi}{L+1}$ is centered between the highest occupied and lowest unoccupied level in a system with N noninteracting fermions with spin as indicated in Fig. 1.

The density of the large Fermi sea in Eq. (4) again shows $4k_F$ density oscillations but in contrast to the true Wigner crystal in Eq. (3) the translational invariance is broken only by the open boundary conditions. There is no spontaneous symmetry breaking in the large Fermi sea since the amplitude in Eq. (4) vanishes in the thermodynamic limit. Nonetheless, the $4k_F$ oscillations indicate a localization of particles near the boundary with a localization length that can be estimated by comparing the amplitude with $2n_0 e^{-2\pi^2\xi^2 n_0^2}$ from Eq. (3). Indeed, the Wigner crystal state and the large Fermi sea are strongly related in 1D. Both can only arise due to strong repulsive interactions and both are spin-incoherent states, which are characterized by a (nearly) degenerate spin sector. The Wigner crystal state has been used as a starting point to derive the concept of a spin-incoherent Luttinger liquid in the limit of very strong long-range interactions by allowing additional fluctuations.[11] On the other hand the large Fermi sea is in fact the *exact* spin-degenerate ground state of the Hubbard model in Eq. (1) in the limit of $U \to \infty$ as can be shown by the Bethe ansatz. *Therefore, both states represent fixed points of infinitely strong interactions, which are unstable for any finite interaction strength.* In this sense the amplitude of the $4k_F$ oscillations plays the role of an order parameter which should be vanishing in the thermodynamic limit in either case. However, in finite systems or at finite energy scales it is in principle possible to observe regions that are dominated by unstable fixed points. In fact, as we will see from the numerical simulations, the order parameter remains finite in systems with open boundary conditions defining a region with dominant spin-incoherent behavior, which is separated by a well-defined crossover.

In the noninteracting limit it is well-known that a finite system exhibits $2k_F$ Friedel oscillations,[8] which are calculated by summing over double occupied standing waves as shown in Fig. 1(a),

$$n(x) = \frac{4}{L+1}\sum_{n=1}^{N/2}\sin^2\left(n\frac{\pi}{L+1}x\right) = n_0 - \frac{\sin(2k_F x)}{(L+1)\sin\left(\frac{\pi}{L+1}x\right)}. \tag{5}$$

It has been predicted that the Friedel oscillations decay slower due to interactions,[12] but as our numerical results show the amplitude is in fact strongly suppressed with increasing U. It must be emphasized here that the $4k_F$ oscillations discussed above are not simply a higher harmonic of the Friedel oscillations, but are an independent interaction effect which in fact competes with the Friedel oscillations as we will see later.

III. BOSONIZATION RESULTS

Using standard bosonization[13] it is possible to predict how finite interactions modify the analytic form of the $2k_F$ and $4k_F$ oscillations. In particular, in the low-energy effective theory after linearization around k_F of the fermion fields $\psi_{\sigma,x} \approx e^{ik_F x}\psi_{R,\sigma} + e^{-ik_F x}\psi_{L,\sigma}$ one can identify the Friedel oscillations as an expectation value of the bosonic operator[12,14,15]

$$\begin{aligned}\mathcal{O}_{LR} &= (e^{i2k_F x}\psi^\dagger_{L,\sigma}(x)\psi_{R,\sigma}(x) + \text{H.c.}) \\ &\propto \sin(2k_F x + \sqrt{2\pi K_c}\varphi_c)\cos(\sqrt{2\pi}\varphi_s).\end{aligned} \tag{6}$$

Here the spin and charge fields represent the mode expansions $\nu = s, c$

$$\varphi_\nu(x) = \frac{Q}{\sqrt{K_\nu}}\frac{x}{L+1} + \sum_{n=1}^{L}\frac{1}{\sqrt{\pi n}}\sin\left(\frac{\pi n}{L+1}x\right)(a_{n,\nu} + a^\dagger_{n,\nu}) \tag{7}$$

according to open boundary conditions $\psi_L(x) = -\psi_R(-x)$.[14] The number counting operator Q does not contribute in ground-state expectation values $\langle Q\rangle = 0$. Using the standard calculations of correlation functions in finite systems[16] the expectation value is determined to be

$$\langle \mathcal{O}_{LR}\rangle \propto \frac{\sin(2k_F x)}{\left[(L+1)\sin\left(\frac{\pi}{L+1}x\right)\right]^{(K_c+1)/2}} \tag{8}$$

up to logarithmic corrections.[17] The interactions change the decay rate of the Friedel oscillations compared to Eq. (5), which appear to be *enhanced* for repulsive interactions $K_c < 1$. However, as we will see, the yet undetermined am-

plitude is strongly suppressed with interactions and at low fillings.

The derivation of the Wigner oscillations from bosonization is more subtle. They arise from interactions because of the Umklapp term in the Hamiltonian density

$$\mathcal{O}_U = g_3(e^{i4k_F x}\psi^\dagger_{R,\uparrow}\psi_{L,\uparrow}\psi^\dagger_{R,\downarrow}\psi_{L,\downarrow} + \text{H.c.}) \propto g_3\cos(4k_F x + \sqrt{8\pi K_c}\varphi_c), \quad (9)$$

where $g_3 \propto U$. In first order perturbation theory this operator induces a density expectation value $\langle n\rangle_U = \langle n\rangle - \langle n\rangle_0$ relative to the unperturbed case

$$\langle n(x)\rangle_U \propto \int_0^L dy \sum_\alpha \frac{{}_0\langle 0|\mathcal{O}_U(y)|\alpha\rangle\langle\alpha|\partial_x\varphi_c(x)|0\rangle_0}{E_\alpha - E_0}, \quad (10)$$

where $|\alpha\rangle$ are all excited states. By using the mode expansion in Eq. (7) it is possible to calculate the expectation values for all bosonic excitations[16] $|\alpha\rangle$ with the result

$$\langle n(x)\rangle_U \propto \frac{g_3 K_c}{v_c}\int_0^L \frac{\sin(4k_F y)g(x,y)}{\left[(L+1)\sin\left(\frac{\pi}{L+1}y\right)\right]^{2K_c}}dy, \quad (11)$$

where $g(x,y) = \Sigma_{m=1}^{L}\frac{1}{m}\sin(\frac{\pi m}{L+1}y)\cos(\frac{\pi m}{L+1}x) \approx \frac{\pi}{2}\theta(y-x)$. Using $\int_x^\infty \sin(4k_F y)y^{-2K_c}dy \approx \cos 4k_F x/4k_F x^{2K_c} + \mathcal{O}(x^{-2K_c-1})$ the integral can be approximated as[18]

$$\langle n(x)\rangle_U \propto \frac{g_3 K_c}{v_c k_F}\frac{\sin\left(4k_F - \frac{\pi}{L+1}\right)x}{\left[(L+1)\sin\left(\frac{\pi}{L+1}x\right)\right]^{2K_c}}. \quad (12)$$

The decay rate for the $4k_F$ oscillations is faster than for the Friedel oscillations in Eq. (8) since $K_c \geq 0.5$ for the Hubbard model. The linear dependence on $g_3/k_F \propto UL/N$ is only accurate to lowest order in perturbation theory but the typical oscillatory behavior and power law will describe the behavior for any U and filling N/L. Alternatively, the *ad hoc* inclusion of $\mathcal{O}_U$ directly in the operator expression for the density is also a valid approach.[5] The explicit derivation from perturbation theory above now provides additional information by indicating an increase in the amplitude with g_3/k_F, i.e., with larger interactions and smaller filling. Note, that both the Friedel oscillations in Eq. (8) and the $4k_F$ oscillations in Eq. (12) have a nonzero expectation value only in systems with open boundary conditions. However, the exact amplitude cannot be derived from bosonization so that numerical calculations have to be used.

IV. NUMERICAL RESULTS

We have implemented a DMRG algorithm[19] for the model in Eq. (1) in order to calculate the local density in finite systems with a given fermion number N. Typical densities at various fillings are shown in Fig. 2 for $U=4t$ and $L=200$, which clearly exhibit the predicted oscillations. Figure 3 shows how the local density at a given filling of $N/L=0.1$ emerges from the slower Friedel oscillations to a Wigner crystal pattern as U increases.

An accurate data analysis is now possible in terms of our analytic predictions from Eqs. (8) and (12),

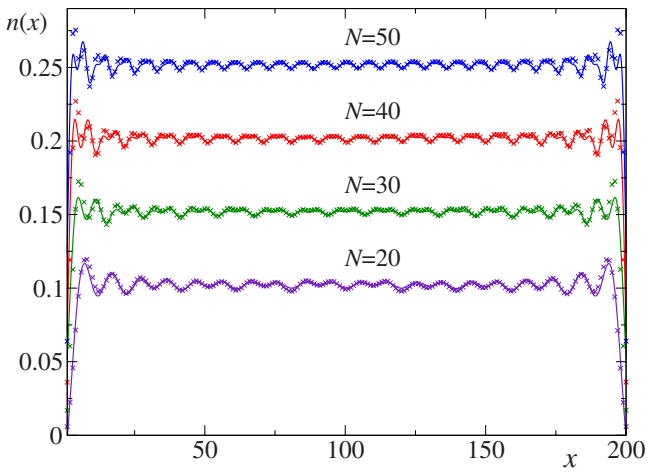

FIG. 2. (Color online) Local density for $U=4t$ and $L=200$ for different fillings showing the Friedel and Wigner crystal oscillations. The solid lines correspond to the theoretical prediction in Eq. (13).

$$n(x) = n_0 - A_1\frac{\sin(2k_F x)}{\left[\sin\left(\frac{\pi}{L+1}x\right)\right]^{(K_c+1)/2}} - A_2\frac{\sin\left(4k_F - \frac{\pi}{L+1}\right)x}{\left[\sin\left(\frac{\pi}{L+1}x\right)\right]^{2K_c}}, \quad (13)$$

where the Friedel amplitude A_1 and the Wigner amplitude A_2 can be determined from fits to the numerical data. For arbitrary interactions $U>0$ and filling N/L the Luttinger parameter $0.5 \leq K_c \leq 1$ can be calculated exactly[5,7,10] as shown in Fig. 5 so that the amplitudes in the middle of the chain A_1 and A_2 are in fact the only two adjustable fitting parameters. For the noninteracting case in Eq. (5) we have $A_1 = \frac{1}{L+1}$ and $A_2 = 0$, which we can use as a test of the numerical accuracy. The uniform density n_0 is fixed by the requirement that $\int n(x)dx = N$ so that it is not an independent fitting parameter (e.g., $n_0 = \frac{N}{L+1}$ for $U=0$).

Figure 2 shows the quality of typical fits to the DMRG data. The oscillations in the middle of the chain are very well represented by the analytical expression (13) while there are

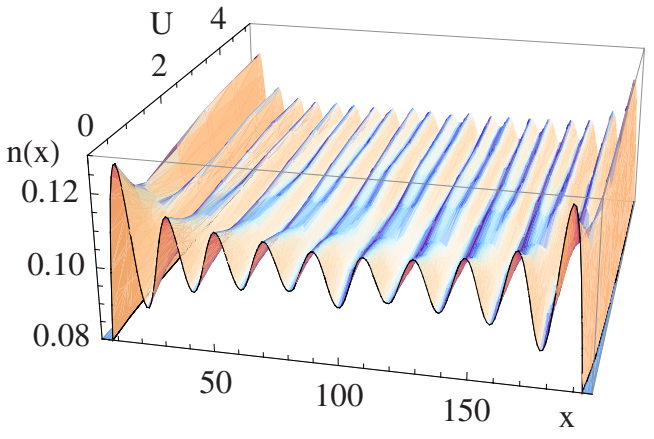

FIG. 3. (Color online) Local density for $N=20$ and $L=200$ showing the crossover from $2k_F$ to $4k_F$ oscillations with increasing interaction strength U.

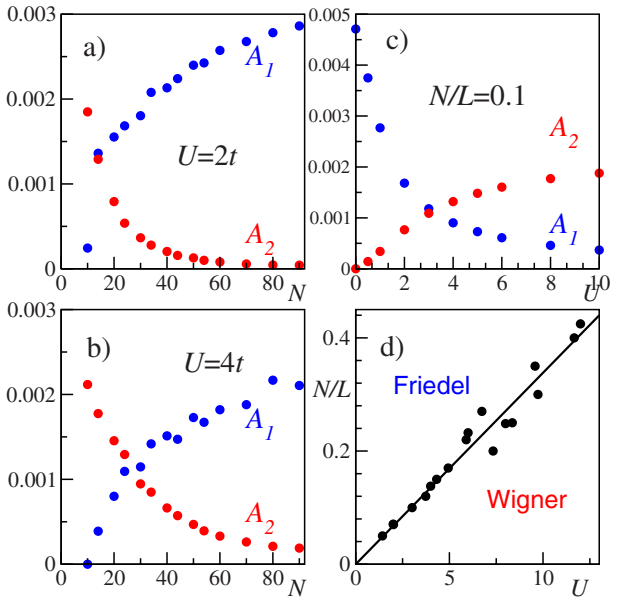

FIG. 4. (Color online) (a)-(c) Crossover of the amplitudes in Eq. (13) (error $\lesssim 10\%$) for $L=200$ from the DMRG data as a function of filling and interaction. (d) Crossover points ($A_1=A_2$) in the $U-N/L$-plane showing the scaling with $N/LU\approx 0.034$ for $L=200$. The solid line separates the Wigner and Friedel regions.

small deviations near the edges. Deviations from Luttinger liquid theory near boundaries have also been observed before in the context of the local density of states.[20] In order to determine the asymptotic amplitudes A_1 and A_2 in the middle of the chain as accurately as possible we have therefore excluded the first few sites near the ends in the fits. The fits are sensitive enough to even confirm the exact values of the wave vectors $2k_F$ and $4k_F-\frac{\pi}{L+1}$ since small deviations of order $\frac{\pi}{L+1}$ already would make the quality of the fits considerably worse.

The results for the Friedel amplitude A_1 and the Wigner amplitude A_2 are shown in Fig. 4 for $L=200$. The amplitudes show a clear crossover from Friedel oscillations to Wigner crystal waves at low filling. Interestingly, the Friedel oscillations are suppressed exactly when the Wigner crystal waves are strong and vice versa. Therefore, it is possible to identify two distinct "regions" of Wigner and Friedel behavior.

From the Luttinger liquid theory it is not *a priori* obvious why Friedel and Wigner oscillations cannot be strong simultaneously but from the discussion in Sec. II it is clear that the Friedel oscillations must compete with the large Fermi sea in Fig. 1 since both states cannot be realized at the same time.

In Fig. 4(d) we have plotted the parameters for which the two amplitudes are equal $A_1=A_2$ for a given length of $L=200$, which we define as the line at which the crossover between the two regions occurs. Interestingly, the crossover occurs along a line of constant N/UL for small fillings (e.g., $N/UL\approx 0.034$ for $L=200$).

The Wigner-type behavior always occurs at low filling or equivalently at large U. At first sight it appears rather counterintuitive that the on-site interaction U should show a stronger effect as the average interparticle distance L/N is increased. This behavior is special to one dimension since

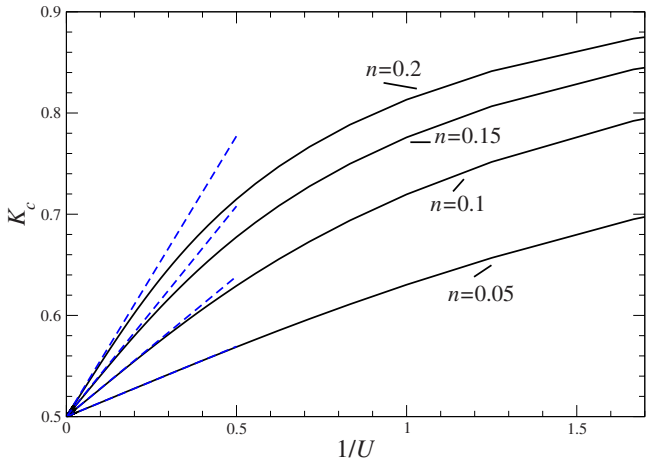

FIG. 5. (Color online) The Luttinger liquid parameter K_c for the Hubbard model from Bethe ansatz compared to the asymptotic form in Eq. (14) for different fillings ($n=N/L$).

the total kinetic energy scales with $(N/L)^3$ at low filling, which becomes always smaller than the total interaction energy, which scales with $(N/L)^2$ as $N/L\to 0$.

The Bethe ansatz equations for the Hubbard model also show scaling behavior in that limit. In particular, we find that the Luttinger parameter is given by the simple expression,

$$K_c \approx 0.5 + \left(\frac{Nt}{UL}\right) 4\ln 2 + \mathcal{O}\left(\frac{N^2}{L^2}, \frac{t^2}{U^2}\right) \qquad (14)$$

in the limit of low filling and large U. This is shown in Fig. 5.

Numerically the scaling behavior for the crossover points in Fig. 4(d) is observed for each length L, separately. However, if the slope of the crossover line N/UL is plotted as a function of length L we observe a clear downturn in the limit of large L as shown in Fig. 6.

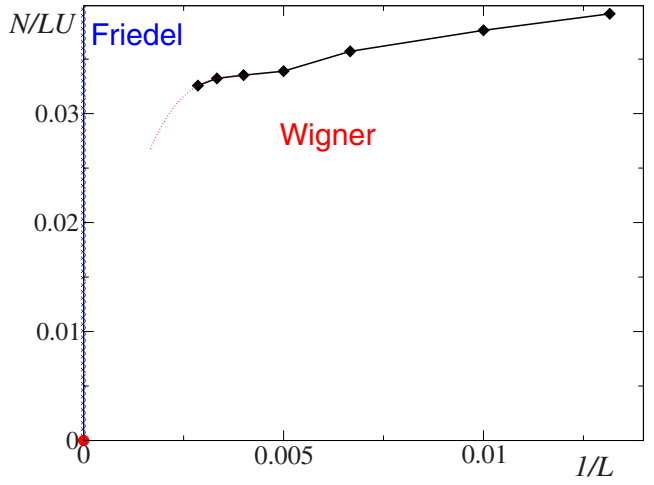

FIG. 6. (Color online) Crossover points N/LU as a function of inverse length $1/L$.

V. CONCLUSIONS

The observed crossover from Friedel to Wigner oscillations is not a true phase transition, which cannot occur in the 1D Hubbard model. Nonetheless, the two regions show clearly different physical behavior. In particular, in the region of $4k_F$ oscillations, the system is characterized by *spin-incoherent* behavior with rather small or vanishing spin correlations according to the arrangement in Fig. 1(b). As outlined in recent works, the spin-incoherent Luttinger liquid shows significantly different physical behavior, especially in regards to transport and tunneling characteristics.[11] The dominance of $4k_F$ oscillations in finite systems appears to be an additional indicator for the onset of spin-incoherent behavior. The particular correlation functions for the local density in finite systems are in fact well suited to study this crossover since the $4k_F$ term in Eq. (12) contains only charge degrees of freedom while the Friedel term in Eq. (8) also contains the spin boson ϕ_s, the amplitude of which is accordingly suppressed in the spin-incoherent regime.

The length dependence of the crossover points N/LU in Fig. 6 violates scaling behavior: For a given density N/L and interaction strength U all parameters in the Luttinger liquid theory (v_c, v_s, K_c) are fixed. Nonetheless, it is still possible to observe a crossover from Wigner to Friedel oscillations as a function of length (moving horizontally in Fig. 6). It is quite surprising that a critical model can cross over to different physical behavior as a function of length only when all relevant parameters are fixed. This remarkable violation of scale invariance is not due to higher order operators such as the well-known logarithmic terms which also give strong corrections to the scaling behavior.[17] Instead, the crossover can be explained by the competition between vastly different velocities in the spin and the charge sectors. Naively, the onset of spin incoherent Luttinger liquid would be expected when the ultraviolet spin cutoff v_s/a becomes comparable to the infrared charge cutoff v_c/L giving a length-dependent crossover. While this may explain the broken scale invariance, this argument does not explain the crossover line in Fig. 6 quantitatively. From the diagram alone it is also not clear that the Friedel region is always stable in the thermodynamic limit $L \to \infty$ but a downturn as indicated by the red dotted line would be expected for larger lengths L.

The arguments presented here are also valid for other Luttinger liquid systems since the competition of spin and charge energy scales is generically always possible as a function of interaction and filling. Therefore, the crossover between the different density oscillations discussed above is a common signature of spin-charge separation in one dimension.

From the experimental side, Luttinger liquid behavior has so far only been seen in very special cases such as carbon nanotubes[21,22] or cleaved edge overgrowth wires.[23] There is some hope now that Luttinger liquid physics can also be realized with ultracold fermionic atoms in nearly ideal geometries formed by optical traps,[24] which would have the advantage that the density distribution discussed here could in principle be detected directly using high-resolution cameras, electron beams,[25] or noise interference.[26] Fermionic gases can already be cooled down to less than $\frac{1}{10}$ of the Fermi energy. The finite temperature will lead to a faster decay of the oscillations from the edges that can be accounted for in the theory.[16] In fact, it would be interesting to perform experiments in a regime where all spin excitations are smaller than the temperature. This would be a perfect realization of the spin-incoherent Luttinger liquid leading to a complete vanishing of the Friedel oscillations while the Wigner oscillations remain. Hard edges can be implemented by focused laser beams or trapped impurity atoms.

In summary, we have systematically analyzed the local density distribution in finite Hubbard chains as a function of filling, interaction strength U, and system size. A combination of bosonization and DMRG calculations allowed a detailed description of the density oscillations in terms of the quantitative formula (13). For small interactions and large fillings $2k_F$ Friedel oscillations A_1 dominate while the Wigner crystal amplitude A_2 remains small. However, for smaller filling or increasing interactions the overall amplitude A_1 of the Friedel oscillations is strongly reduced while A_2 grows. This signals the crossover to a different physical region, which is described by a spin-incoherent large Fermi sea with no double occupancy of spin-up and spin-down fermions. The density oscillations we have described here are an accessible feature to study the crossover toward the spin-incoherent Luttinger liquid in detail, e.g., using ultracold fermionic gases in 1D optical traps.

ACKNOWLEDGMENTS

We are thankful for useful discussions with Sebastian Reyes. This work was supported by the DFG and the State of Rheinland-Pfalz via the SFB/Transregio 49 and the MATCOR school of excellence.

[1] E. Wigner, Phys. Rev. **46**, 1002 (1934).
[2] V. V. Deshpande and M. Bockrath, Nat. Phys. **4**, 314 (2008).
[3] R. Jördens, N. Strohmaier, K. Günter, H. Moritz, and T. Esslinger, Nature (London) **455**, 204 (2008).
[4] I. Bloch, J. Dalibard, and W. Zwerger, Rev. Mod. Phys. **80**, 885 (2008).
[5] H. J. Schulz, Phys. Rev. Lett. **64**, 2831 (1990); **71**, 1864 (1993).
[6] G. A. Fiete, J. Qian, Y. Tserkovnyak, and B. I. Halperin, Phys. Rev. B **72**, 045315 (2005); E. J. Mueller, *ibid.* **72**, 075322 (2005).
[7] F. H. L. Essler, H. Frahm, F. Göhmann, A. Klümper, and V. E. Korepin, *The One-Dimensional Hubbard Model* (Cambridge University Press, Cambridge, England, 2005).
[8] J. Friedel, Nuovo Cimento **7**, 287 (1958).
[9] G. Bedürftig, B. Brendel, H. Frahm, and R. M. Noack, Phys. Rev. B **58**, 10225 (1998).

[10] M. Bortz and J. Sirker, J. Phys. A **39**, 7187 (2006).
[11] K. A. Matveev, Phys. Rev. Lett. **92**, 106801 (2004); V. V. Cheianov and M. B. Zvonarev, *ibid.* **92**, 176401 (2004); G. A. Fiete, Rev. Mod. Phys. **79**, 801 (2007).
[12] R. Egger and H. Grabert, Phys. Rev. Lett. **75**, 3505 (1995).
[13] For a review see S. Eggert, *Theoretical Survey of One Dimensional Wire Systems*, edited by Y. Kuk, S. Hasegawa, and Q. K. Xue (Sowha, Seoul, 2007), p. 13; arXiv:0708.0003 (unpublished).
[14] S. Eggert and I. Affleck, Phys. Rev. B **46**, 10866 (1992); Phys. Rev. Lett. **75**, 934 (1995); M. Fabrizio and A. O. Gogolin, Phys. Rev. B **51**, 17827 (1995); S. Eggert, H. Johannesson, and A. Mattsson, Phys. Rev. Lett. **76**, 1505 (1996).
[15] S. Rommer and S. Eggert, Phys. Rev. B **62**, 4370 (2000).
[16] A. E. Mattsson, S. Eggert, and H. Johannesson, Phys. Rev. B **56**, 15615 (1997); S. Eggert, A. E. Mattsson, and J. M. Kinaret, *ibid.* **56**, R15537 (1997).
[17] T. Giamarchi and H. J. Schulz, Phys. Rev. B **39**, 4620 (1989).
[18] The wave vector shift $-\frac{\pi}{L+1}x$ is taken from Eq. (4).
[19] S. R. White, Phys. Rev. Lett. **69**, 2863 (1992); Phys. Rev. B **48**, 10345 (1993); U. Schollwöck, Rev. Mod. Phys. **77**, 259 (2005).
[20] I. Schneider, A. Struck, M. Bortz, and S. Eggert, Phys. Rev. Lett. **101**, 206401 (2008).
[21] M. Bockrath, D. H. Codben, J. Lu, A. G. Rinzler, R. E. Smalley, L. Balents, and P. L. McEuen, Nature (London) **397**, 598 (1999).
[22] J. Lee, S. Eggert, H. Kim, S. J. Kahng, H. Shinohara, and Y. Kuk, Phys. Rev. Lett. **93**, 166403 (2004).
[23] O. M. Auslaender, A. Yacoby, R. de Picciotto, K. W. Baldwin, L. N. Pfeiffer, and K. W. West, Science **295**, 825 (2002).
[24] A. Widera, S. Trotzky, P. Cheinet, S. Folling, F. Gerbier, I. Bloch, V. Gritsev, M. D. Lukin, and E. Demler, Phys. Rev. Lett. **100**, 140401 (2008).
[25] T. Gericke, C. Utfeld, N. Hommerstad, and H. Ott, Laser Phys. Lett. **3**, 415 (2006); T. Gericke, P. Wartz, D. Reitz, T. Langen, and H. Ott, Nat. Phys. **4**, 949 (2008).
[26] M. Greiner, O. Mandel, T. W. Hänsch, and I. Bloch, Nature (London) **419**, 51 (2002).